ADVANCED OPTICAL MATERIALS

Supporting Information

for *Adv. Optical Mater.,* DOI: 10.1002/adom.202102113

Deep Convolutional Neural Networks to Predict Mutual Coupling Effects in Metasurfaces

Sensong An, Bowen Zheng, Mikhail Y. Shalaginov, Hong Tang, Hang Li, Li Zhou, Yunxi Dong, Mohammad Haerinia, Anuradha Murthy Agarwal, Clara Rivero-Baleine, Myungkoo Kang, Kathleen A. Richardson, Tian Gu, Juejun Hu, Clayton Fowler, and Hualiang Zhang**

Supporting Information

Title: Deep convolutional neural networks to predict mutual coupling effects in metasurfaces

Sensong An[1,2], Bowen Zheng[1], Mikhail Y. Shalaginov[2], Hong Tang[1], Hang Li[1], Li Zhou[1], Yunxi Dong[1], Mohammad Haerinia[1], Anuradha Murthy Agarwal[2,3], Clara Rivero-Baleine[4], Myungkoo Kang[5], Kathleen A. Richardson[5], Tian Gu[3], Juejun Hu[2,3], Clayton Fowler[1,], Hualiang Zhang[1,*]*

1. Near field mutual couplings in different metasurfaces

By comparing the near-field distributions between electric field simulations of meta-atoms with identical neighbors and differing neighbors, considerable deviations inside the center meta-atom can be observed in all four cases.

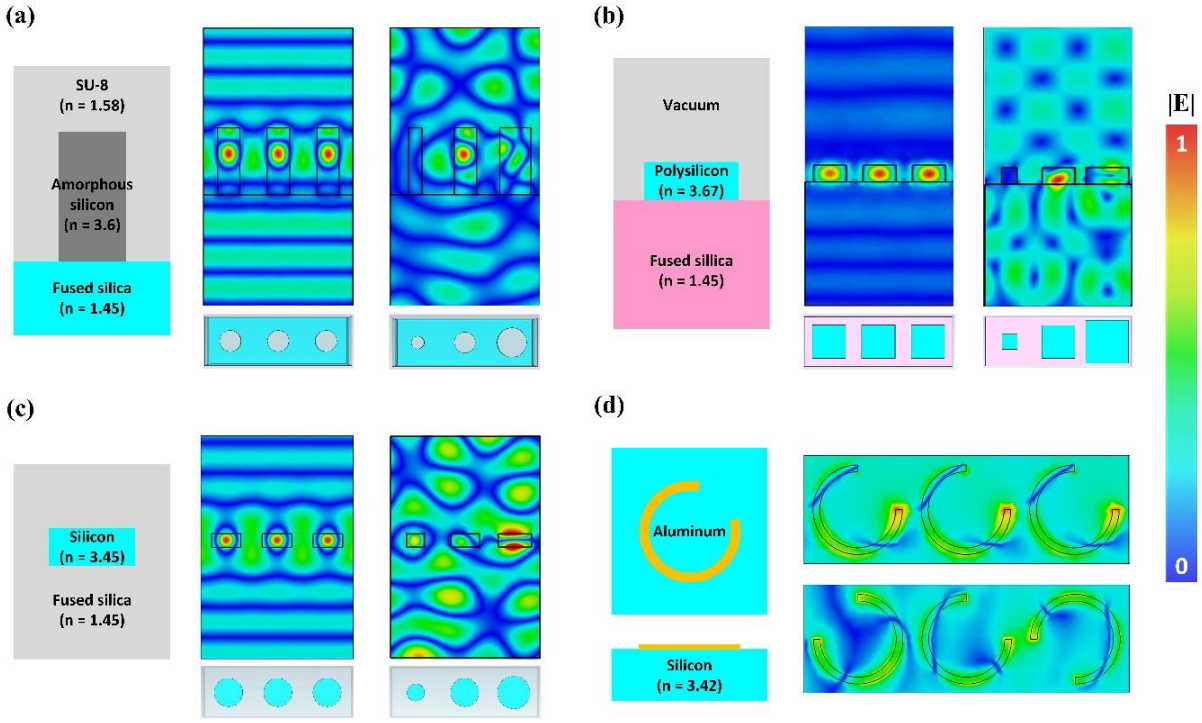

Fig. S1. Simulated near-field electric field distribution of meta-atoms with identical and different neighbors. Structures and materials of each meta-atom model are shown on the subplots (left). The meta-atoms in the center of each 3 meta-atom groups are placed with identical

(middle) and different (right) neighbors. In each case of non-identical neighbors, the perturbing effects of near-field coupling cause significant change in the field distribution inside the central meta-atom. Numerical modelling of the mea-atom geometries: **(a)** Ref. [7], **(b)** Ref. [9], **(c)** Ref. [8] and **(d)** Ref. [6], were performed using a full-wave simulation tool CST Microwave Studio.

2. Detailed simulation setups to derive local responses

The transmissive all-dielectric metasurface design being considered in this work is showing in Fig. S2a. Considering that mutual coupling effects decrease with distance, it is necessary to determine the number of neighboring meta-atoms that needs to be considered in each simulation. To do so, we randomly generated a group of meta-atoms that consisted of a target meta-atom surrounded by 10 differing meta-atoms on each side (Fig. S2b). We initially simulated the structure with a periodic boundary condition and gradually increased the number of neighbors in the simulation (Fig. S2c) to examine how the local response of the target meta-atom changes. We treat the local response with all 10 neighbors on each side as a reference point with zero error, because improvements in accuracy are marginal with the inclusion of additional neighbors beyond this point. We repeated this experiment on 1,000 different groups of meta-atoms and calculated the average phase and amplitude error. As shown in Fig. S2d, the simulation results of target meta-atoms with a periodic boundary (hereinafter referred to as "periodic responses") have significant amplitude and phase mean absolute error (MAE) of 0.33 and 59.14 degrees compared to when the number of neighboring meta-atoms (N) is 10. As the number of neighboring meta-atoms increases, the error gradually decreases. The large error values in Fig. 1e are caused by the abrupt changes in phase gradients that can occur in randomly arranged meta-atoms. According to the results, even a single neighboring meta-atom on each side of the target considerably improves its EM response's accuracy, which is in accordance with our predictions. To strike a balance

between simulation accuracy and optimization difficulty (as well as data collection costs), we selected N = 4 during the data collection process.

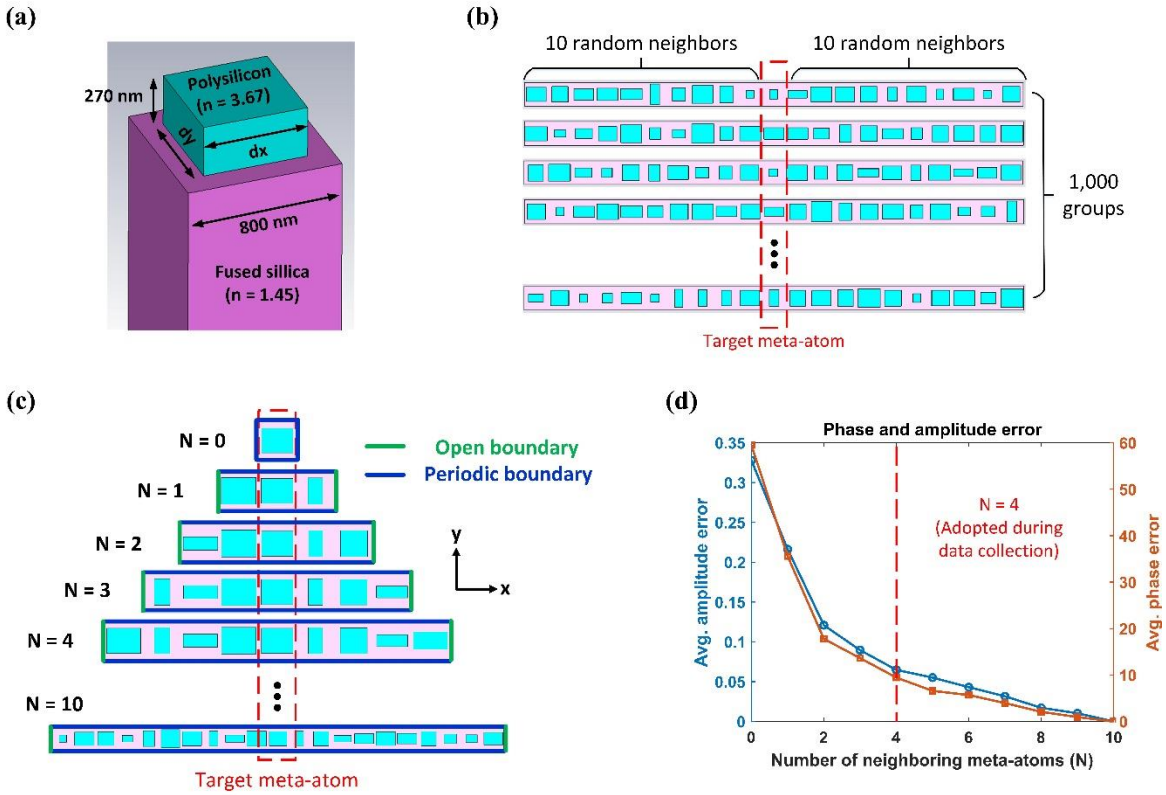

Figure S2. Simulation setups. (a) Schematic of a meta-atom represented as a silicon nanoblock on top of fused silica substrate. (b) 1,000 randomly generated target meta-atoms (inside the red contour) surrounded by 10 random neighbors on each side. (c) Different numbers of neighboring meta-atoms (N) were considered to derive accurate EM responses for each target meta-atom. (d) The average amplitude and phase error as a function of N. N = 0 represents the results derived with periodic boundaries. N = 4 was adopted during the data collection process.

3. Optimization of a full-size high NA metalens

To further demonstrate that this approach is compatible with full size metasurface designs, a high NA metalens (NA = 0.72) composed of 200 meta-atoms was also designed and optimized. The focal length of this larger metalens is set to be 50 wavelengths (77.5 μm). After 500 iterations of optimization (finished in 200 minutes), the local response, target response and phase error are calculated and plotted for each meta-atom in the initial design (Fig. S3a) and optimized design (Fig. S3b) are calculated and plotted. This optimization process not only improved the focusing efficiency, but also fixed the focal length shifting problem caused by accumulating phase errors in the initial design (Fig. S3c). The average phase error of the optimized design is 14.6°, largely reduced compared to the 65.3° phase error of the initial design, which increased the electric field intensity at the focal spot from 6.5 V/m to 8.2 V/m.

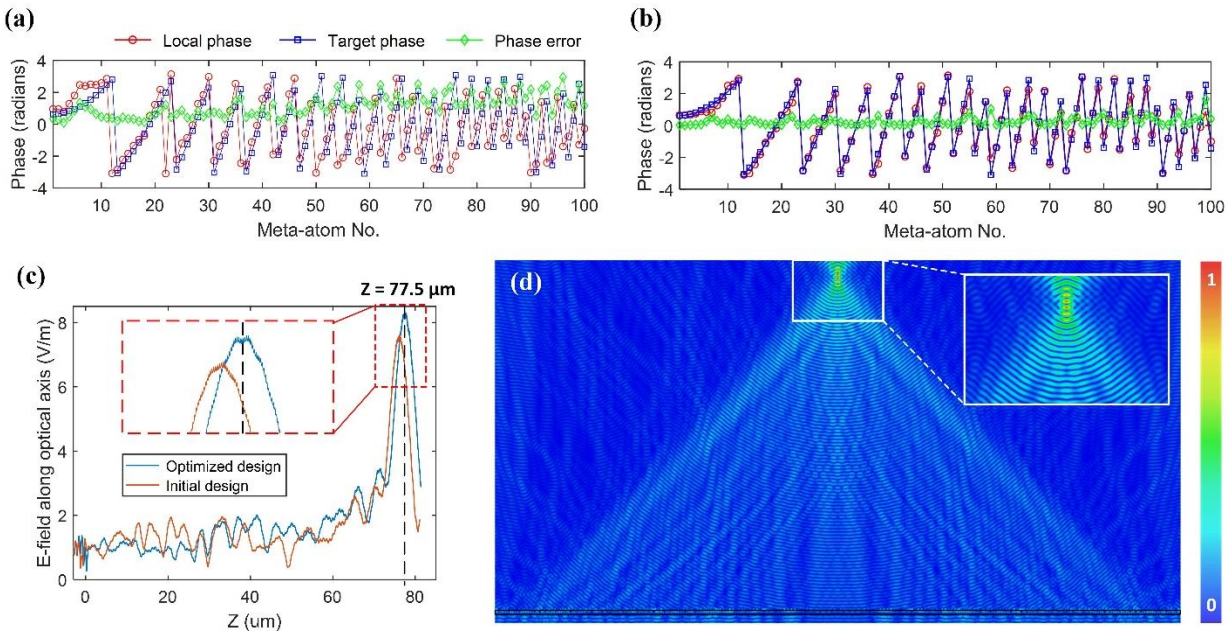

Figure S3. Optimization of a larger metalens composed of 200 meta-atoms. Target phase (blue), local phase (red) and phase error (green) of each meta-atom in (a) the initial and (b) the optimized design. (c) Simulated electric field magnitude along the optical (Z) axis, x-polarized for the initial design (red) and the optimized design (blue). The inset contains a magnified view of the electric

field near the focal spot. (d) Simulated electric field (real part) of the optimized design and magnified view of the electric field near the focal spot (inset).

4. Data collection setup for high-index freeform metasurface

High index meta-atoms confine EM fields more strongly than low index meta-atoms and thus are less prone to mutual coupling. Therefore, we only consider the influence of 2 neighbors on each side during the data collection process (Fig. S4), which provides the same level of accuracy (amplitude error less than 0.07, phase error less than 11°).

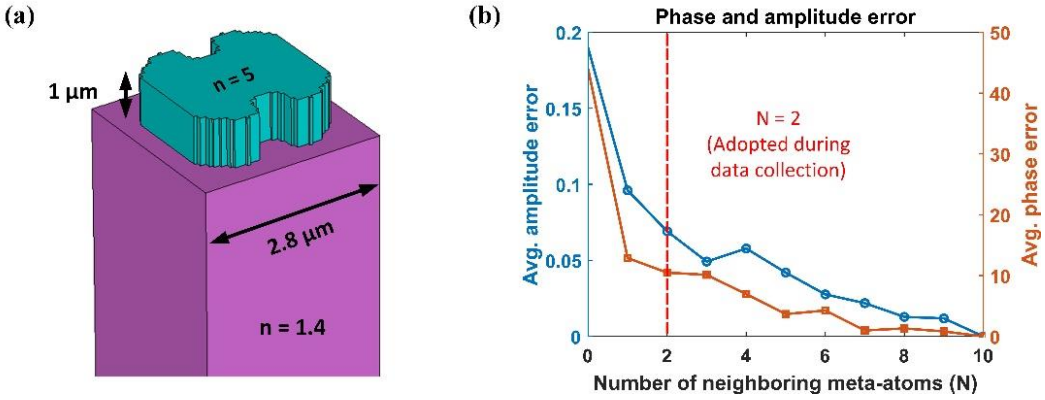

Figure S4. Data collection setup for freeform meta-atoms. (a) Schematic of a freeform meta-atom composed of a high-index material sitting on top of a low-index substrate. (b) The amplitude and phase MAE for a specified number of non-identical neighboring meta-atoms on each side, N. N = 0 represents the results derived with periodic boundaries. N = 2 was adopted during the data collection process.

5. Extend to 2-dimensional cases

To further demonstrate the versatility of the proposed approach, we collected more data based on the same metasurface platform (1-μm-thick film of n = 5 dielectric material placed on an n=1.4 dielectric substrate, with 2.8 μm period and 5.45 μm wavelength). In this case we consider the influence of 2 neighbors on both x and y directions during the data collection process (Fig. S5). Following the same simulation procedure presented in the supplemental document section II, we collected another 40,000 groups of 2D data, which were later used during the training process (70% for training and 30% for validation). The whole data collection process took approximately 10 days using an 8-node computer cluster.

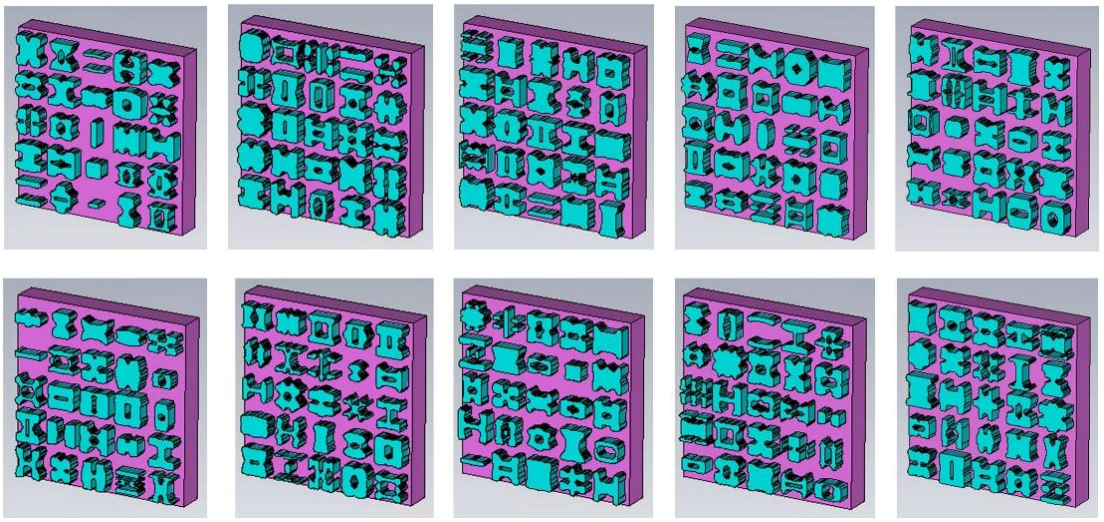

Figure S5. Some randomly-generated 2D meta-atom samples for data collection process.

As shown in Fig. S6a, the network architecture was slightly modified to accommodate the changed input dimensions (from a 320 × 64 to 320 × 320). One more convolution layer was added to the network to further shrink the size of the input to the fully-connected layers. Once fully trained, the final accuracy (3×10^{-5} for the training set and 9×10^{-5} for the test set) was comparable to the previous 1D network accuracy. Similarly, 6 results (Fig. S5b) were randomly selected from the test dataset for demonstration purpose.

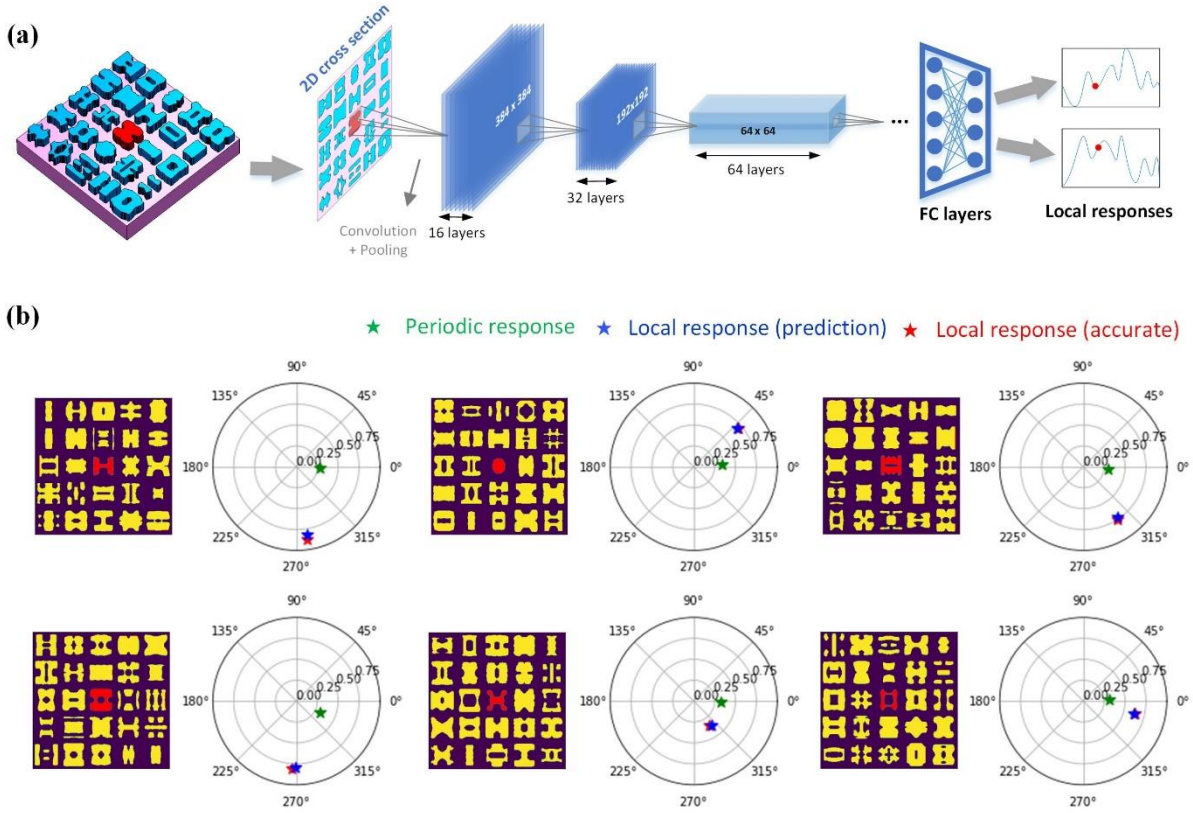

Figure S6. (a) Network architecture of the modified PNN that deals with 2D mutual coupling problems. (b) Phase-amplitude polar diagrams showing six groups of EM responses from randomly selected test set geometries. The target meta-atoms are marked in red, while the neighbors are marked in yellow. Periodic-boundary responses are labeled with green stars, while local responses predicted with PNN and calculated with CST are denoted with blue and red stars, respectively.

6. Time efficiency analysis

Table S1. The time taken for the data collection and network training

Data collection process	Time cost (1 group)	No. of data	Total data collection time (with 8 workstations in parallel)	Network training time
In Fig. 3 (Rectangle, 1D)	~70 s	200,000	~11 days	~10 hours
In Fig. 6 (Freeform, 1D)	~150 s	100,000	~12 days	~10 hours
In Fig. S6 (Freeform, 2D)	~700 s	40,000	~20 days	~ 12 hours

The most time-consuming process of this deep learning approach is the data collection process. The time costs for all data collection processes are shown in Table S1. As indicated by the numbers, the simulation time of different structures is usually proportional to their electrical sizes, hence the time taken for 1D structures will be shorter than 2D structures, and larger structures (meta-atoms with more neighbors considered) will be longer than smaller structures. Also, metasurfaces with higher refractive index usually take longer to model, considering their larger effective electrical volume. As we have pointed out the manuscript, the meta-atoms with high refractive index are usually less prone to the mutual coupling effects, meaning less number of neighbors are needed to be considered during the data collections. Furthermore, the data collection process could be further accelerated by using more workstations running in parallel or using GPUs (in which case we measured a three-time efficiency improvement).